RSC Advances

ROYAL SOCIETY OF CHEMISTRY

www.rsc.org/advances

CO_2 Hydrogenation to Dimethyl Ether over CuO-ZnO-Al_2O_3/HZSM-5 Prepared by Combustion Route

Yajing Zhang[1], Debao Li,[1] Sujuan Zhang[1], Kangjun Wang[1], Jing Wu[1,*]

[1] College of Chemical Engineering, Shenyang University of Chemical Technology, Shenyang 110142, PR China

Abstract

CuO-ZnO-Al_2O_3/HZSM-5 catalysts were prepared and characterized by XRD, BET, N_2O titration, H_2-TPR, FESEM and NH_3-TPD techniques. CuO-ZnO-Al_2O_3 catalysts were obtained by a simple and fast urea-nitrate combustion method and then mixed physically with HZSM-5 to perform one step synthesis of dimethyl ether (DME) from carbon dioxide (CO_2) hydrogenation. The results showed that the grain size and copper surface areas of the catalysts were highly affected by the amount of urea in the preparation, and the catalytic performances were consequently influenced. CO_2 conversion of 30.6% and DME yield of 15% over the optimal catalyst were obtained by controlling the molar ratio of urea to metal nitrate. The work will benefit for the rational design of new catalysts suitable for CO_2 utilizations.

Key words: Caron dioxide; Hydrogenation; Dimethyl ether; combustion method;

1. Introduction

One of the major challenges of our time is to find efficient solutions beyond our diminishing fossil fuels resources and the grave environmental consequences of excessive combustion of carbon-containing fuels and their products [1, 2]. A good solution is chemical recycling of CO_2 to renewable, environmentally carbon neutral

* Corresponding author. E-mail address: wujing7275@163.com.Phone: +86-24-89383902.

fuels, for example, methanol and DME [3-5]. Synthesis of DME from CO_2 hydrogenation has attracted great interest because: (1) DME can be used as a good propellant and a coolant; (2) DME is proposed as a clean fuel due to its near-zero smoke, less engine noise, low NOx emissions. (3) One step synthesis of DME from CO_2 hydrogenation reaction can break the thermodynamic restriction that exists for methanol synthesis and consequently improve the CO_2 conversion [6].

Currently, a hybrid catalyst, composed by both methanol synthesis and methanol dehydration catalysts, is generally developed for one step synthesis of DME from CO_2 hydrogenation. For the methanol synthesis catalyst, Cu-based metal oxides are usually CuO–ZnO–Al_2O_3 and CuO–ZnO–ZrO_2, some catalysts include promoters such as SiO_2, Y_2O_3, Ga_2O_3, and so on [7-10]. It is reported that the factors suggested to influence the activity of catalyst include Cu surface area, Cu dispersion, and reducibility of CuO to metallic Cu, Cu species, Cu grain size, Cu crystal planes exposed, lattice strain, crystal phase of the support, complex method, besides the composition [11]. However, the structure-activity relationships for DME synthesis catalysts are not fully understood. And it is well known that the structure of the catalyst is highly affected by preparation method. Therefore, investigation on the influence of the preparation method on the catalytic performance is essential. Co-precipitation method, which usually employs alkaline carbonate as a precipitating agent, is the most common commercially method used to prepare Cu-based catalyst. However, this method is time-consuming because ageing step is necessary. Additionally, a lot of water has to be used for removing the residual alkaline,

otherwise the alkaline will produce a negative effect on the catalytic performance of the catalyst. Therefore, it is necessary to develop fast and low cost methods for the catalyst preparation [12, 13]. Recently, a simple, fast and low cost combustion method based on the principles of propellant chemistry was employed to synthesize metal oxides powders, which have attracted great efforts because high-purity, homogenous metal oxide powders with higher crystalline degree and surface areas can be obtained from the process [14, 15]. Mao's group reported CuO-ZnO-ZrO_2 catalyst for methanol synthesis from CO_2 hydrogenation was prepared via a combustion method and the catalyst showed higher activity [16]. Shi et al. prepared metallic Cu/ZnO catalysts by a sol–gel auto-combustion method and a higher activity was obtained for low-temperature of methanol synthesis from CO_2-containing syngas [17, 18]. Guo et al. reported CuO-ZnO-ZrO_2 catalyst for methanol synthesis from CO_2 hydrogenation was prepared by a glycine-nitrate combustion and revealed the relationship between physiochemical properties and the fuel content [19].

Here CuO-ZnO-Al_2O_3/HZSM-5 catalysts were prepared for DME synthesis from CO_2 hydrogenation. CuO-ZnO-Al_2O_3 catalysts prepared by the urea-nitrate combustion method, and then physically mixed with HZSM-5 by grinding to form CuO-ZnO-Al_2O_3/HZSM-5 catalysts. The effect of the amount of urea used as fuel on catalytic properties of the catalysts has been investigated, aiming to enhance conversion of CO_2, yield of DME and better understand the structure-catalytic performance relationship of CuO-ZnO-Al_2O_3/HZSM-5 catalysts.

2. Experimental Section

2.1 Catalyst preparation

In a typical procedure, analytical pure $Cu(NO_3)_2 \cdot 3H_2O$, $Zn(NO_3)_2 \cdot 6H_2O$ and $Al(NO_3)_3 \cdot 9H_2O$ were dissolved into a certain amount of deionized water, in which the molar ratio of Cu^{2+}, Zn^{2+}, Al^{3+} meets the formula of $(CuO)_{0.48}(ZnO)_{0.37}$ $(Al_2O_3)_{0.15}$. Then urea solution was dropwise added to the nitrate solution. The resulting mixture was transferred to crucibles. Finally, the crucibles were transferred to a muffle furnace preheated at 673 K. The solution ignited spontaneously and finished in very short time. And the powder was heated at 673 K for 4 hours to remove other impurities. At last, a fluffy black powder was obtained and recorded as CZA. The urea addition was set from 30% to 150% of the stoichiometric amount which is 2.17 moles for 1 mol CZA catalyst according to propellant chemistry [20]. Then the CZA was mixed with HZSM-5 (mass ratio of 2) by grinding in an agate mortar to prepare the hybrid catalysts. And the HZSM-5 was purchased from Catalyst Plant of Nankai University (China) with SiO_2/Al_2O_3 ratio of 50. Then the hybrid catalysts were pressed to a thin piece, crushed, and sieved to obtain the particles in 20-40 mesh, the catalysts were denoted as 30CZAH, 40CZAH, 50CZAH, 75CZAH, 100CZAH, 150CZAH, respectively.

2.2 Catalyst testing

Activity and selectivity measurements of the catalysts were carried out in a continuous-flow fixed-bed reactor made of stainless steel (i.d.=10 mm). Prior to the measurements, the catalysts were reduced in a stream of 10% H_2/N_2 at 573 K for 3 h under atmospheric pressure. Then the reactor was cooled to 353 K, and reactant gas

flow was introduced, then the pressure was raised to 3.0 MPa and the reaction temperature was raised to 543 K. The exit line from the reactor to the gas-sampling valve was heated to prevent condensation. The products were analyzed on line with a gas chromatograph (SP2100A) equipped with both a TCD (for CO and CO_2, GDX-101 connected with Porapak T column) and a FID (for CH_4, CH_3OH and CH_3OCH_3, Porapak Q column). Conversion and selectivity values were calculated by internal standard and mass conservation method.

2.3 Catalyst characterization

XRD measurements were performed on a Rigaku D/max 2500pc X-ray diffractometer with Cu-Kα radiation (λ=1.54156 Å) at a scan rate of 4° min^{-1} at 50 kV and 250 mA. The grain size was calculated from the XRD spectra by using the Scherrer equation.

FESEM images were obtained on a JEOL-6490 field-emission scanning electron microscope with accelerating voltage of 20 kV.

BET surface areas were measured by N_2 adsorption at 77 K using a Quantachrome Autosorb 1-C. Before measurements, samples were degassed under vacuum at 573 K for 4 hours.

H_2-TPR was also conducted to examine the catalyst reducibility. 50 mg of the catalyst was heated in He at 673 K for 60 min, followed by cooling to room temperature. The temperature was then raised in 50 mL/min of 10% H_2/Ar using a ramp rate of 10 K/min to 823 K. H_2 consumption was detected using TCD.

NH_3-TPD was conducted on chemisorptions (ChemBET 3000) from 373 to 873 K.

The catalyst (100 mg) was heated to 673 K and maintained for 30 min, then the temperature was cooled to 373 K, following that a 6 vol. % NH_3/Ar mixture stream was introduced for adsorption (60 min). After adsorption, the examined catalyst was flushed with helium stream (30mL/min) for 60 min to remove the weak adsorbed NH_3, and then it was heated from 373 to 873 K at a rate of 10 K/min. The TPD signal was recorded.

Copper surface areas (S_{Cu}) were measured by a nitrous oxide titration method as described in elsewhere [4, 21].

3. Results and discussion

3.1 catalytic performance

The catalytic properties of the reduced CZAH catalysts for CO_2 hydrogenation to DME were tested. The major product was DME, and the side products included methanol, CO and methane. The amount of methane was less than 1% and can be neglected. The conversion of CO_2, the selectivities of DME and methanol are shown in Table 1. It can be found that the conversion of CO_2 and the yield of DME first increase and then decrease with the increasing urea amount, and the change trends are similar to those of the S_{BET} and S_{Cu}. As shown in Table 1, 40CZAH shows the highest CO_2 conversion, DME selectivity and DME yield. For synthesis of DME from CO_2 hydrogenation over Cu-based catalysts, metallic Cu is believed to be an active phase. It is evident that the activity and Cu surface area are strongly correlated as indicated by the volcano-shaped dependence of activity on Cu surface area according to our results. In addition, grain size of active species also plays an important role in

determining the performances of the catalysts [20], and the catalytic activity increases with decreasing grain size of Cu species. The result shows the catalytic performances of the catalysts for DME synthesis from CO_2 hydrogenation are highly dependent on their structure. Furthermore, the results reveal that, among all the catalysts examined here, the one prepared with 40% of the stoichiometric amount of fuel (urea) exhibits the highest activity for the conversion of CO_2 and favors the formation of the desired DME, which can be ascribed the largest surface copper area (S_{Cu}) and the smallest copper grain size (d_{Cu}) after reduction.

For comparison, the CZA catalyst with the same composition was prepared by an oxalate co-precipitation method according to the reference [23]. And then CZAH catalyst was also prepared by physical mixing method，i.e. grinding CZA catalyst and HZSM-5 in an agate mortar according to the mass ratio of 2:1. Under the same reaction conditions, the conversion of CO_2 was 27.1% and the yield of DME was 12.9%. The result indicates that the most efficient 40CZAH catalyst prepared by the combustion method exhibits higher catalytic performance compared with the one prepared by the oxalate co-precipitation method.

3.2 The structure of the catalysts

Figure 1 shows the XRD patterns of the CZAH catalysts. The strong and sharp peaks observed in Figure 1 confirm the catalysts are all well crystallized. For 150CZAH and 100CZAH, the diffraction peaks appear at 35.5°, 38.7°, 48.7°, 53.4°, 58.2°, 61.5°, 66.2°, 72.3° and 74.9° can be indexed to CuO phase (tenorite, JCPDS 48-1548), the peaks at 31.7°, 34.3°, 36.1°, 47.4°, 56.5°, 62.8° and 67.8° can be

ascribed to ZnO phase (JCPDS 65-3411), and the peaks at 31.2°, 36.8°, 59.3°, 65.1° and 77.3° can be ascribed to $CuAl_2O_4$ (JCPDS 33-0448) or $ZnAl_2O_4$ (JCPDS 74-1136) phase. For 75CZAH, 50CZAH, 40CZAH and 30CZAH catalysts, no diffraction peaks of $CuAl_2O_4$ or $ZnAl_2O_4$ phases can be detected. For all catalysts, the peaks of Al_2O_3 were not observed, indicating Al_2O_3 were amorphous or well dispersed in the catalyst body phase; and the peaks appear in the 2θ range of 21-25° belong to HZSM-5 (JCPDS 44-0003). With the decreasing of urea amount from 150% to 40% of stoichiometry, the intensities of the diffraction peaks of CuO and ZnO weaken and the width of the peaks broaden gradually, and even some peaks belong to CuO phase disappear. This indicates the crystallization degree decreases with the decreasing urea amount. However, it is interesting to note that the diffraction peaks of 30CZAH become stronger and sharper compared with those of 40CZAH, indicating the crystallization degree increases again if further decrease the urea amount, meanwhile, the result can be confirmed from the values of BET surface areas (S_{BET})，surface copper areas (S_{Cu}) and the grain sizes of CuO (d_{CuO}) of the two catalysts. It can be explained from the point view of reaction temperature during the combustion process [16]. The urea could play two roles during the combustion process, on one hand, it provides heat for raising the reaction temperature for igniting the solution spontaneously; on the other hand, it releases gases which may transfer some heat and lower the combustion temperature [24-25]. These two roles compete with each other. When the urea amount is too small (for example, 30CZAH), less gases comes out from the process, resulting in a relatively higher reaction temperature than more urea

amount are included (for example, 40CZAH).

The XRD patterns of the reduced catalysts are shown in Figure 2. It can be found that the XRD patterns of the catalysts show the diffraction peaks at 2 θ values of 43.3 °, 50.4 ° and 74.1°,which can be indexed to the crystal planes of (111), (200) and (220) of metallic copper phase, respectively (JCPDS 04-0836). No diffraction peaks belong to CuO phase can be detected in all the catalysts, suggesting all CuO species have been reduced to copper. While for the 150CZAH and 100CZAH catalysts, the diffraction peaks of $CuAl_2O_4$ and/or $ZnAl_2O_4$ still present in the patterns after reduction, indicating it can not be reduced at the temperature. The existence of spinel ($CuAl_2O_4$ and/or $ZnAl_2O_4$) could be one of the reasons why the 150CZAH and 100CZAH have smaller surface copper areas (S_{Cu}) compared with the others, which thus decrease the catalytic performances of the two catalysts.

The specific surface areas and the calculated grain sizes of the catalysts using Scherrer's equation are listed in Table 1. As shown in Table 1, the S_{BET} first slightly increases from 30CZAH to 40CZAH and then decreases gradually from 40CZAH to 150CZAH with the increasing urea amount. The changing trend of the copper surface area is the same as that of S_{BET}, while opposite to the change trend of the d_{Cu} of the catalysts, the growth of crystal grain and/or the agglomeration of particle with the increase combustion temperature (it changes with the amount of urea) are responsible for the changes of S_{BET}, S_{Cu} and d_{Cu}. It is interesting to note that for all catalysts, the grain size of CuO phase is smaller than that of ZnO phase. Shimokawabe et al. claimed this phenomenon indicated CuO may be deposited dispersedly on the ZnO

particles thus improving the active interfacial region or active sites [26]. This result is consistent with the studies of Li et al. [17]. The catalyst 40CZAH shows the maximum S_{BET} of 140.1 m^2/g , S_{Cu} of 15.6 m^2/g and the minimum copper crystal size of 20.8 nm, which could be the reasons account for the best catalytic performance of the catalyst.

Moreover, to better understand the relationships between the surface copper areas (S_{Cu}) and the catalytic properties of the CZAH catalysts, turnover frequency (TOF) were also calculated using the values of S_{Cu} and the result was shown in Figure 3. Here TOF was defined as the number of reacted CO_2 molecules per surface metallic copper atom per second. The TOF of reacted CO_2 decreases as the S_{Cu} increases, as shown in Figure 3. The observation indicates the characteristics of structural sensitive reaction of direct synthesis of DME from CO_2. This result is in good agreement with previous report on the Cu-based catalysts for methanol synthesis from CO_2 [19]. However, the result is different from those reported by Bae et al. on reaction of single step synthesis of DME from syngas over the modified CuO-ZnO-Al_2O_3/ferrierite catalysts [27, 28]. Bae et al. concluded that the reaction was structural insensitive over their CuO-ZnO-Al_2O_3/ferrierite catalysts. The difference between Bae's and ours could be attributed to different raw materials (syngas and CO_2, respectively) and different catalysts systems were employed. Furthermore, combined with the results listed in Table 1, it can be concluded that TOF decreases with the decreasing urea amount from 150% to 40% of stoichiometry, but TOF increases again if further decreasing urea amount to 30%, which indicates TOF is influenced by the variation of

urea amount used in catalysts preparation.

3.3 The reducibility of the catalysts

In order to investigate the reducibility of the catalysts, H_2-TPR was performed, and the measurement results are shown in Figure 4. As shown in Figure 4, TPR profiles of the catalysts exhibit one broad peak of H_2 consumption. Obviously, all the peaks are asymmetric, indicating an overlapping of two reduction processes [24]. To get deep insight into the TPR results, the broad peaks are deconvoluted into two peaks, which are denoted as α and β peaks, respectively. And the peak position and their contributions are summarized in Table 2. Under the experimental conditions used in this study, all metal oxides except CuO in these catalysts are nonreducible. Consequently, α and β peaks occur in the range of 478 to 533 K in the TPR profiles, implying the presence of different CuO species with slight differences in ease of reducibility. The similar results have also been reported for other Cu-based catalysts, α peak (the low-temperature reduction peak) was attributed to the reduction of highly dispersed CuO and β peak (the high-temperature reduction peak) was attributed to the reduction of bulk CuO [29]. The TPR profiles show that the intensities of α peak become weaker gradually, while the intensities of β peak become stronger with the increasing urea amount. At the same time, the β peaks maxima shift to higher temperature. These results imply that increasing urea amount in preparation does not facilitate CuO reducibility. It is also noted that there is no reduction peaks belong to the spinel phase ($CuAl_2O_4$) on the TPR profiles of 150CZAH and 100CZAH catalysts, as confirmed from the XRD patterns of reduced catalysts (Figure 2). The TPR

findings (Table 2) also show that the relative contribution of α peak to the whole TPR pattern first increases and the decreases with the increasing urea amount, and a maximum of 58.2% is reached for 40CZAH catalyst. This may be another reason account for the best performance of 40CZAH catalyst [18].

3.4 Morphologies of the CuO–ZnO–Al_2O_3 catalysts

The morphologies of the CuO–ZnO–Al_2O_3 catalysts were observed by FESEM, and the results were shown in Figure 5. The amount of urea has an obvious influence on the morphologies of CuO–ZnO–Al_2O_3 (CZA) catalysts. For the 40CZA catalyst (Figure 5a and 5b), a lot of curly fluffy flake-like aggregates are observed, which seem like loose sponges composed of many small uniform particles (average size is less than 100 nm). This morphology possibly facilitates the adsorption and diffusion of the reactant molecules and therefore the 40CZAH shows higher activity than the others [30]. With the increasing amount of urea in the preparation process, the average size of the particles of CuO–ZnO–Al_2O_3 catalyst becomes larger, as evidently confirmed from figure 5c, d (75CZA) and 5e, f (150CZA). For 75CZA, some compact appearances can also be observed besides flake-like morphology, indicating a denser structure of the catalyst. The FESEM image of the 150CZA shows no flake-like morphology but lots of ball-like agglomerates. The magnified image of 150CZA indicates the ball-like agglomerates are assembled by particles with diameters of about 500 nm (Figure 5f). Furthermore, some balls even grow together and form a chain-like structure, and this may decrease dispersion of copper oxide. It can also be speculated that the surface area of CZA component will decrease with the increasing

urea (fuel) due to the growing average particle size. The FESEM result is consistent with that of BET surface areas. The clear morphological differences between these catalysts suggest the amount of urea (fuel) used in the combustion process is the key factor determines the structure and consequently the catalytic performance of the catalysts.

3.5 **Surface acidity of the CuO–ZnO–Al_2O_3/HZSM-5 catalysts**

The acidity of the CuO–ZnO–Al_2O_3/HZSM-5 catalysts and pure HZSM-5 were characterized by NH_3-TPD, as depicted in Figure 6. Two desorption peaks can be observed on pure HZSM-5 profile, and the peak located in the range 400-500 K (denoted as α peak) can be attributed to the weak acidic sites, while the peak located within the range of 550-750 K (denoted as β peak), belong to strong acid sites [31, 32]. After mixing CuO–ZnO–Al_2O_3 catalysts with HZSM-5, peaks α still kept at the same temperature, however, their areas became much smaller, which indicated that much lower concentration for weak acid sites on the surface of the CuO–ZnO–Al_2O_3/HZSM-5 catalysts; while peaks β shifted to the lower temperature and their areas also became smaller, indicating both the strength and concentration of the strong acid sites decreased, which facilitated for the adsorption of CO_2 [33]. In addition, for all CZAH catalysts, intensities of peaks β were not same, peak positions of some catalysts (30CZAH, 40CZAH, 50CZAH) are lower than those of the others (75CZAH, 100CZAH, 150CZAH), which may be another reason why the former show better performance (shown in Table 1). Compared with pure HZSM-5 curve, it was found a new peak appeared on CZAH catalysts in the range of 525 to 550 K

(denoted as γ peak), which could be attributed to the middle strong acid sites of HZSM-5 [34]. On pure HZSM-5 curve, peak γ may be covered by peak β and therefore only two peaks were observed. The NH_3-TPD results demonstrate the acidities of CZAH catalysts were also influenced by the urea amount used during CZA catalysts preparation.

4 Conclusions

A series of CuO–ZnO–Al_2O_3/HZSM-5 catalysts were prepared by the urea–nitrate combustion and mechanical methods. The results show that the amount of fuel (urea) has a great influence on the structure of the catalysts. With addition urea amount of 40% stoichiometry, smaller CuO and Cu grain size, higher BET and copper surface areas, lower reduction temperature were obtained, which led to a better performance of the CuO–ZnO–Al_2O_3/HZSM-5 (40CZAH) catalyst. More than 30% CO_2 conversion and 15% yield of DME over the optimal 40CZAH catalyst were obtained.

Acknowledgement

The authors thank Liaoning Science and Technology Department Foundation (No.2007223016), Liaoning Educational Department Foundation (L2011065), Liaoning Educational Department Foundation (L2013161),Shenyang Science and Technology Department Foundation (No.F11-264-1-76) for financial support.

References

[1] G. A. Olah, A. Goeppert, G. K. Surya Prakash, *J. Org. Chem.*, 2009, **74**, 487–498.

[2] T. Sakakura, J. C. Choi, H. Yasuda. *Chem. Rev.*, 2007, **107**, 2365-2387.

[3] G. Centi, S.Perathoner, *Catal. Today,* 2009, **148**, 191-205.

[4] X. An, Y. Z. Zuo, Q. Zhang, D. Z. Wang, J. F. Wang, *Ind. Eng. Chem. Res.*,2008, **47**, 6547-6554.

[5] Q. Zhang, Y. Z. Zuo, M. H. Han, J. F. Wang, Y. Jin, F. Wei, *Catal. Today*, 2010, **150**, 55-60.

[6] G. Bonura, M. Cordaro, L. Spadaro, C. Cannilla, F. Arena, F. Frusteri, Appl. Catal. B: Environ. 140-141 (2013) 16-24.

[7] J. Sloczyński, R. Graowski, P. Olszewski, A. Kozlowska, J. Stoch, M. Lachowska, J. Skrzypek, Appl. Catal. A: Gen 310 (2006) 127–137.

[8] T. Inui, H. Hara, T. Takeguchi, J. B. Kim, *Catal. Today*, 1997, **36**, 25−32.

[9] P. Clancy, J. P. Breen, J. R. H. Ross, *Catal. Today*, 2007, **127**, 291−294.

[10] K. P. Sun, W. W. Lu, F. Y. Qiu, S. W. Liu, *Appl Catal A: Gen*., 2003, **252**, 243-249.

[11] S. Natesakhawat, J. W. Lekse, J. P. Baltrus, et al. *ACS Catal*.,2012, **2**, 1667-1676.

[12] F. Zha, J. Ding, Y. Chang, J. F. Ding, et al. *Ind. Eng. Chem. Res.*, 2012, **51**, 345–352.

[13] T. Witoon, T. Permsirivanich, W. Donphai, A. Jaree, M. Chareonpanich, *Fuel. Process. Technol.*, 2013, **116**, 72-78.

[14] Y. Y. Li, L. H. Xue, L. F. Fan, Y. W. Yan, *J Alloy Compd*, 2009, **478**, 493-497.

[15] Y. W. Jiang, S. G. Yang, Z. H. Hua, H. B. Huang, *Angew. Chem. Int. Ed.*, 2009, **48**, 8529-8531.

[16] X. M. Guo, D. S. Mao, S. Wang, G. S. Wu, G. Z. Lu, Catal. Commun., 2009, **10**, 1661–1664.

[17] L. Shi, C. Y. Zeng, T. J. Wang, N. Tsubaki, *Catal. Sci. Technol.*, 2012, **2**, 2569-2577.

[18] L. Shi, K. Tao, R. Q. Yang, F. Z. Meng, C. Xing, N. Tsubaki, *Appl Catal A: Gen.*, 2011,401 , 46-55.

[19] X. M. Guo, D. S. Mao, G. Z. Lu, S. Wang, G. S. Wu, *J. Catal.*, 2010, 271, 178-185.

[20] S.R. Jain, K.C. Adiga, V.R. Pai Verneker, *Combust. Flame*, 1981, **40**, 71–79.

[21] F. Arena, K. Barbera, G. Italiano, G. Bonura, L. Spadaro, F. Frusteri, *J. Catal.* 2007, **249**, 185–194.

[22] C. Baltes, S. Vukojevic, D. Schuth, *J Catal.*, 2008, **258**, 334−344.

[23] Y. J. Zhang, J. L. Deng, J. Wu, K. J. Wang, S. J. Zhang, K. Zhang, *J Mol Catal (China)*, 2013, **27**, 43-48.

[24] R.D. Purohit, B.P. Sharma, K.T. Pillai, A.K. Tyagi, *Mater. Res. Bull.*, 2001, **36**, 2711–2721.

[25] X. M. Guo, D. S. Mao, G. Z. Lu, S. Wu, G. H. Wu, Catal. Commun., 2011, **12** , 1095-1098.

[26] M. Shimokawabe, H. Asakawa, N. Takezawa N, *Appl. Catal*., 1990, **59**, 45-58.

[27] J. W. Jung, Y. J. Lee, S. H. Um, P. Yoo, D. H. Lee, K. W. Jun, J. W. Bae, *Appl. Catal. B: Environ.*, 2012, **126**, 1-8.

[28] Y. J. Lee, M. H. Jung, J. B. Lee, K. E. Jeong, H. S. Roh, Y. W. Suh, J. W. Bae, *Catal. Today*, 2013, http: //dx.doi.org/10.1016/j. catod. 2013. 11. 015.

[29] M.D. Rhodes, A.T. Bell, *J. Catal*., 2005, **233**, 198-209.

[30] S. G. Li, H. J. Guo, C. R. Luo, H. R. Zhang, L. Xiong, X. D. Chen, L. L. Ma, *Catal. Lett.*, 2013,**143**, 345-355.

[31] C. V. Hidalgo, H. Itoh, T. Hattori, M. Niwa, Y. Murakami, *J. Catal*., 1984, **85**, 362-370.

[32] J. Kang, K. Cheng, Q. Zhang, J. Ding, W. Hua, et al. *Angew. Chem*., 2011, 123, 5306-5309.

[33] L. X. Zhang, Y. C. Zhang, S. Y. Chen. *Appl. Catal*. A: Gen., 2012, **415-416**, 118-123.

[34] L. J.Lobree, I. C. Hwang, J. A. Reimer, A. T. Bell, *J. Catal*., 1999, **186**, 242-253.

Figure captions:

Table 1 Physicochemical properties and performances of the $CuO–ZnO–Al_2O_3$/HZSM-5 catalysts.

Table 2 Temperature of reduction peaks and their contributions to the TPR pattern over the $CuO–ZnO–Al_2O_3$/HZSM-5 catalysts

Figure 1 XRD patterns of the $CuO–ZnO–Al_2O_3$/HZSM-5 catalysts: (a) 30CZAH; (b) 40CZAH; (c) 50CZAH; (d) 75CZAH; (e) 100CZAH; (f) 150CZAH;

Figure 2 XRD patterns of the reduced $CuO–ZnO–Al_2O_3$/HZSM-5 catalysts: (a) 30CZAH; (b) 40CZAH; (c) 50CZAH; (d) 75CZAH; (e) 100CZAH; (f) 150CZAH;

Figure 3 The relationship between the TOF of reacted CO_2 and the surface copper areas (S_{Cu}). Reaction conditions: T = 543 K; P = 3.0 MPa; CO_2: H_2 = 1:3; GHSV = 4200 h^{-1} ;

Figure 4 H_2-TPR profiles of the $CuO–ZnO–Al_2O_3$/HZSM-5 catalysts.

Figure 5 Low magnification and high magnification FESEM images of the $CuO–ZnO–Al_2O_3$ catalysts (CZA): (a, b) 40CZA; (c, d) 75CZA; (e, f) 150 CZA.

Figure 6 NH_3-TPD profiles of pure HZSM-5 and the catalysts (a) HZSM-5; (b) 30CZAH; (c) 40CZAH; (d) 50CZAH; (e) 75CZAH; (f) 100CZAH; (g) 150CZAH;

Table 1 Physicochemical properties and performances of the $CuO–ZnO–Al_2O_3$/HZSM-5 catalysts.

Catalysts	S_{BET} (m^2/g)	S_{Cu}[a] (m^2/g)	D^b_{XRD} (nm)			Conversion Of CO_2 (%)	Selectivity (%)		DME yield %
			d_{CuO}	d_{ZnO}	d_{Cu}		DME	CH_3OH	
30CZAH	130.1	7.0	16.7	27.9	20.9	28.1	44.3	11.2	12.5
40CZAH	140.1	15.6	14.6	20.8	20.8	30.6	49.2	10.4	15.1
50CZAH	134.3	11.1	17.3	29.8	21.1	28.8	46.1	13.1	13.3
75CZAH	133.2	6.1	22.3	30.9	25.6	26.8	38.0	9.3	10.2
100CZAH	94.5	5.8	30.4	37.5	35.4	24.8	37.3	9.6	9.3
150CZAH	93.9	3.2	39.7	52.3	48.6	17.2	42.7	9.4	7.4

Reaction conditions: T = 543 K; P = 3.0 MPa; CO_2: H_2 = 1:3; GHSV = 4200 h^{-1} ;

[a] Determined by nitrous oxide titration method;

[b] Diffraction spectra at 2θ=38.7° for CuO, 31.7° for ZnO, and 43.3° for Cu.

Table 2 Temperature of reduction peaks and their contributions to the TPR pattern over the CuO–ZnO–Al_2O_3/HZSM-5 catalysts

Samples	T_α/K	T_β/K	$A_\alpha/(A_\alpha+A_\beta)$ [a] %
30CZAH	485	502	44.1
40CZAH	483	504	58.2
50CZAH	484	506	44.3
75CZAH	489	507	43.8
100CZAH	490	517	38.7
150CZAH	502	525	32.1

[a] A_α and A_β represent the area of α and β peak, respectively ;

Graphical Abstract

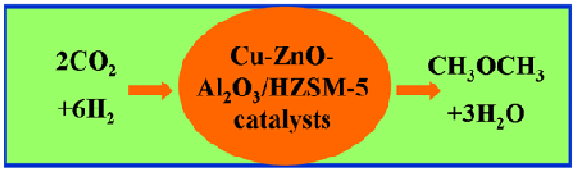

Text:

$CuO\text{-}ZnO\text{-}Al_2O_3$ were prepared by a combustion method and then mixed with HZSM-5 to perform direct synthesis of DME from CO_2.

Figure 1 XRD patterns of the CuO–ZnO–Al_2O_3/HZSM-5 catalysts: (a) 30CZAH; (b) 40CZAH; (c) 50CZAH; (d) 75CZAH; (e) 100CZAH; (f) 150CZAH;

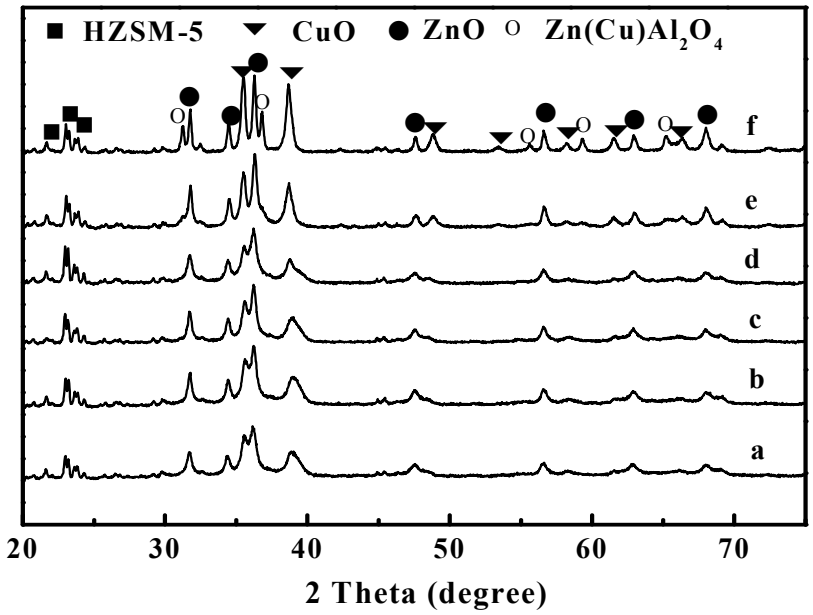

Figure 2 XRD patterns of the reduced CuO–ZnO–Al_2O_3/HZSM-5 catalysts: (a) 30CZAH; (b) 40CZAH; (c) 50CZAH; (d) 75CZAH; (e) 100CZAH; (f) 150CZAH;

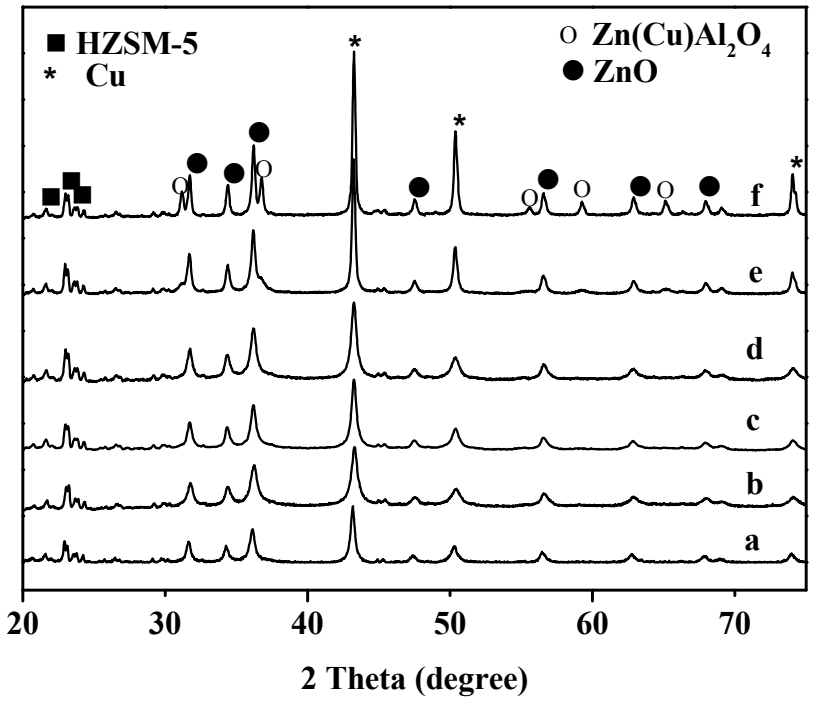

Figure 3 The relationship between the TOF of reacted CO_2 and the surface copper areas (S_{Cu}). Reaction conditions: T = 543 K; P = 3.0 MPa; CO_2: H_2 = 1:3; GHSV = 4200 h^{-1} ;

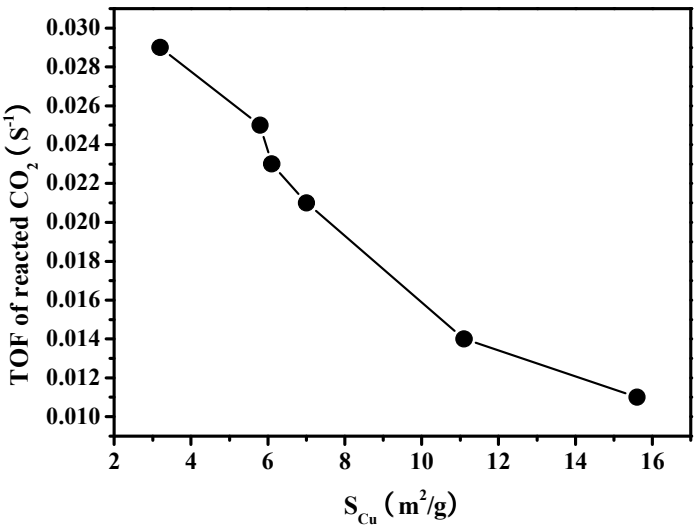

Figure 4 H_2-TPR profiles of the CuO–ZnO–Al_2O_3/HZSM-5 catalysts.

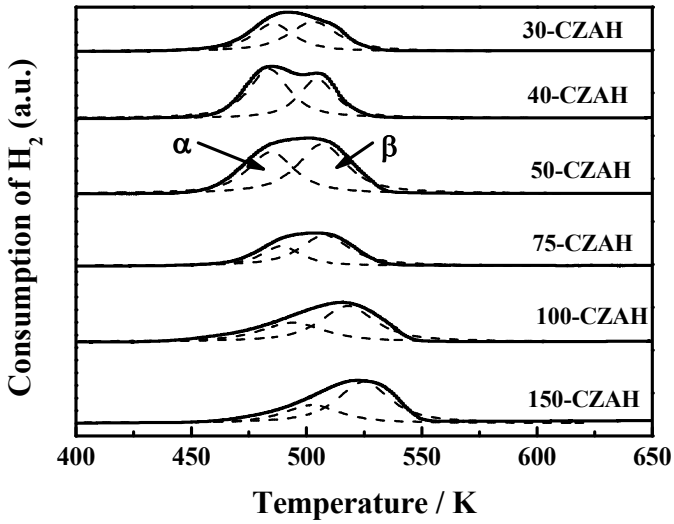

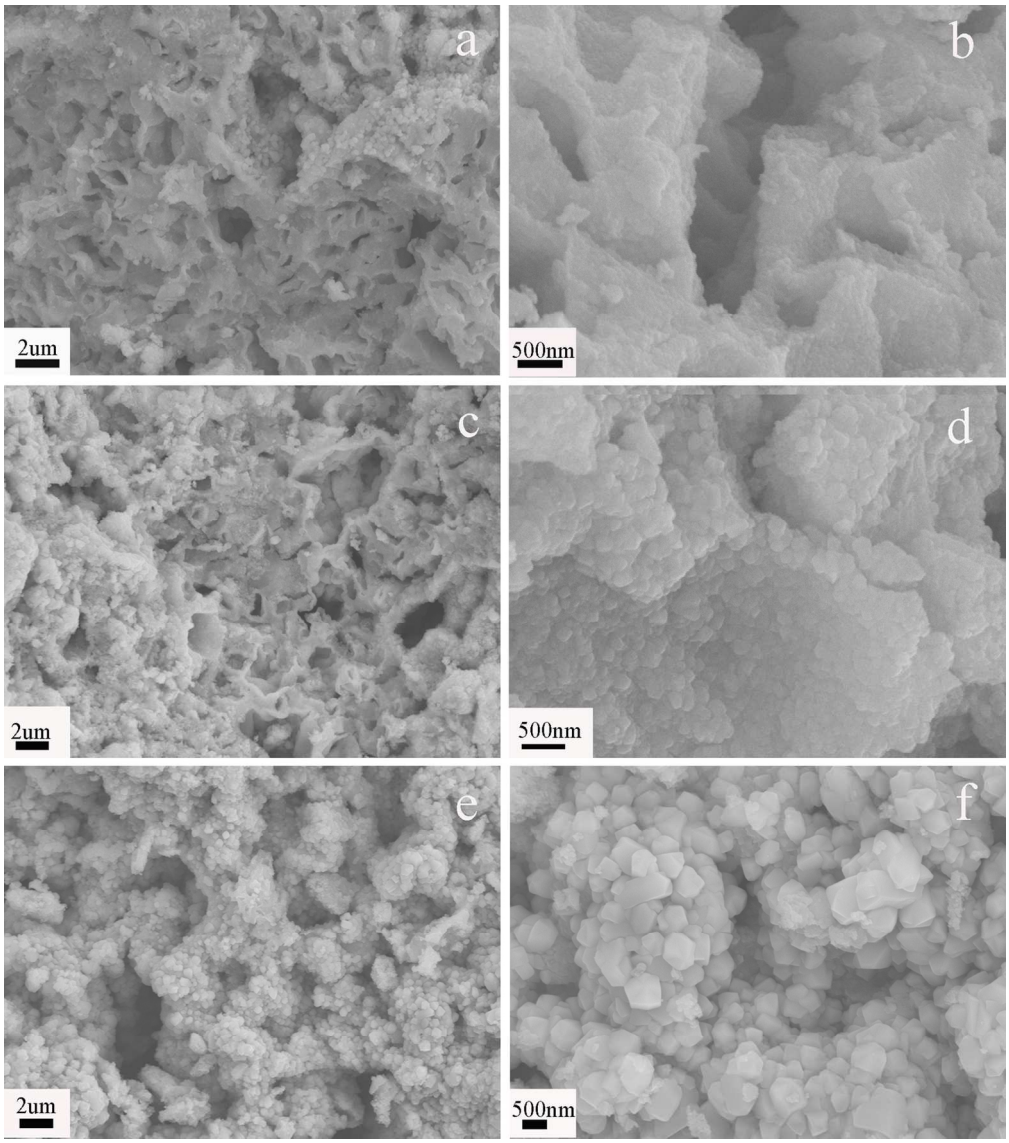

Figure 5 Low magnification and high magnification FESEM images of the CuO–ZnO–Al2O3 catalysts (CZA): (a, b) 40CZA; (c, d) 75CZA; (e, f) 150 CZA.
136x154mm (300 x 300 DPI)

Figure 6 NH_3-TPD curves of HZSM-5 and the catalysts: (a) HZSM-5; (b) 30CZAH; (c) 40CZAH; (d) 50CZAH; (e) 75CZAH; (f) 100CZAH; (g) 150CZAH;